JOURNAL OF MATERIALS SCIENCE 27 (1992) 6387–6390

Strain-rate and temperature-dependent stress–strain curves of Sn–Pb eutectic alloy

K. KAWASHIMA, T. ITO, M. SAKURAGI*
Department of Mechanical Engineering, Nagoya Institute of Technology, Gokisocho, Showaku, Nagoya 466, Japan

Tensile tests on cast Sn–Pb eutectic alloy have been carried out at 25, 100, 140, 170 °C and several strain rates ranging from 7×10^{-3}–$7 \times 10^{-5}\,s^{-1}$. The stress–strain curves obtained were strongly dependent on strain rate and temperature. Under the conditions tested, higher strain-rates gave a higher stress–strain curve and a larger strain at fracture. The tensile strength may be expressed by a power function of strain rate whose exponent and coefficient are governed by a kind of Arrhenius' equation. The nominal stress–strain curves showed significant work softening due to diffuse necking; however, the true stress–strain curve exhibited slight work softening. Thus the elastic perfectly viscoplastic model can be applied to the solder.

1. Introduction

Solder is indispensable for connecting electronic devices with printed circuit boards. Nowadays many electric and electronic units are mounted on automobiles. Different from electric appliances used indoors, solder joints mounted on automobiles are used under more severe temperature conditions ranging from −30 °C–140 °C, for example. To ensure reliability of these solder joints, the mechanical properties of solder under service conditions must be known. Many works have been reported on the fatigue strength of solders (e.g. [1, 2]), creep behaviour [3–6] and thermal cycling tests of soldered joints [7]. In order to analyse stress or strain distribution of solder joints subjected to mechanical or thermal loading, the stress–strain curves under various loading conditions should be known. However, no stress–strain curves of solder alloy can be found in a reference book of stress–strain curves [8]. A few stress–strain curves [6, 9, 10] have been reported; however, they refer only to tests at room temperature. It is important to clarify the mechanical behaviour at high temperature, because the solder is expected to exhibit highly viscoplastic behaviour, i.e. the stress–strain curve depends on strain rate and temperature.

In this paper, we present experimental results of uniaxial tension tests of cast Sn–Pb eutectic alloy at constant temperatures of 25, 100, 140 and 170 °C under strain rates of 7×10^{-5}, 7×10^{-4}, 1.8×10^{-3} and $7 \times 10^{-3}\,s^{-1}$. The effects of temperature and strain rate on the stress–strain curve are discussed and an empirical expression of the constitutive relation dependent on strain rate and temperature is given.

2. Experimental procedure

The material used in the experiment was commercially available Sn–Pb eutectic solder (Sn 62.3, Pb 37.7 wt %). The extruded solder, as-received, was melted and cast into a mould made of stainless steel in our laboratory. The tensile specimen, 5 mm thick, shown in Fig. 1, was machined from a plate-like ingot. Fig. 2 shows the micro-structure of the specimen, which is very similar to that of solder joints manufactured with reflow soldering. The specimen was elongated by a horizontal screw-driven testing machine equipped with a heating unit, which is composed of heating elements of a contact type sandwiched between thin aluminium plates. These plates prevent the distortion of the specimen at high temperature. The temperature of the specimen within the gauge length was controlled within 3 °C by adjusting the electric current of each heating element.

The load applied to the specimen and the relative displacement of the specimen between grips, measured by the displacement transducer, were stored in a digital memory at a suitable time interval. The axial strain was evaluated by dividing the relative displacement by the effective gauge length, which was determined from the ratio of the relative displacement mentioned above to the reading of a strain gauge cemented on the specimen, based on a calibration test done at room temperature. This method was used because direct strain measurement was difficult due to the use of a contact type heating unit.

The tensile tests were conducted at 25, 100, 140 and 170 °C under nominal strain rates of 7×10^{-5}, 7×10^{-4}, 1.8×10^{-3} and $7 \times 10^{-3}\,s^{-1}$.

3. Results and discussion

Figs 3–6 show the nominal stress–strain curves at 25, 100, 140 and 170 °C, respectively. These curves are the outputs of the nominal stress and strain, processed with a personal computer. At 25 °C, tests were repeated twice for each strain rate. The two stress–strain

* *Present address*: Makita Electric Works Ltd, Anjyo 446, Japan.

0022–2461

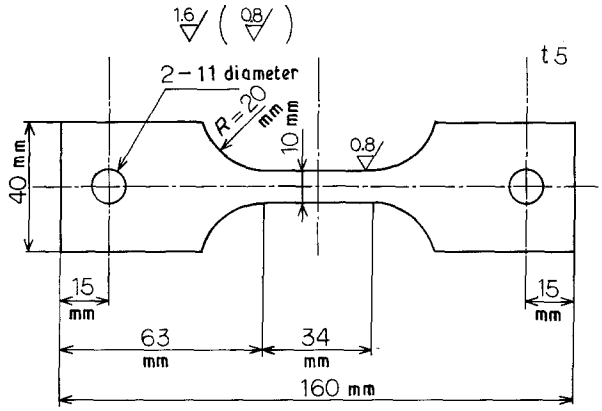

Figure 1 Geometry of the test specimen.

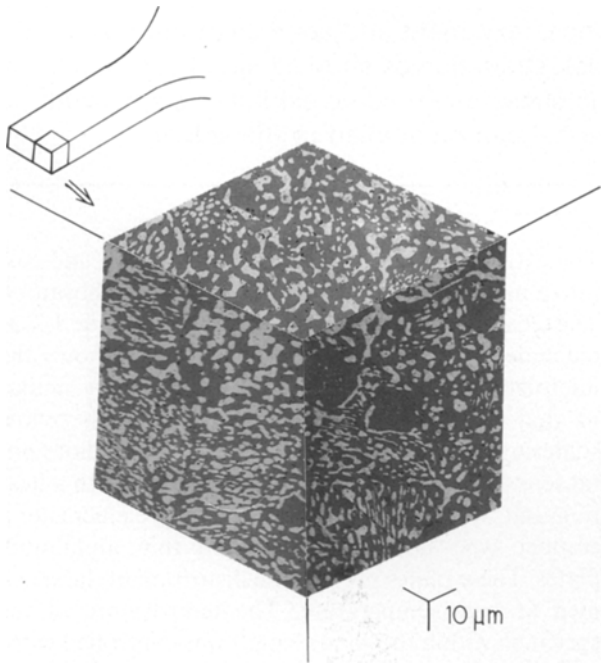

Figure 2 Scanning electron micrograph.

curves of the same strain–rate are very close, therefore, the mechanical property of the cast solder is stable.

At each temperature, the higher strain rate gave rise to a higher stress–strain curve. The tensile strength was attained at a few per cent strain, and thereafter the nominal stress gradually decreased due to diffuse necking. The latter was significant at high temperature. Generally, strain at fracture was also larger at high strain rates. The scattering of the strain at fracture is attributed to the random distribution of small voids and impurities formed during the casting process. The stress–strain curves of strain rate $7 \times 10^{-4}\,s^{-1}$ in Fig. 3 are very similar to that obtained for the eutectic Sn–Pb solder at room temperature and $\dot{\varepsilon} = 1.5 \times 10^{-4}\,s^{-1}$ by Satoh *et al.* [9].

The effect of strain rate on the tensile strength is shown in Fig. 7. In this range of strain rate, the tensile strength is expressed by formula

$$\sigma = A\dot{\varepsilon}^{1/N} \quad (1)$$

where the coefficients A and N depend on temperature. Different from the usual assumption of the

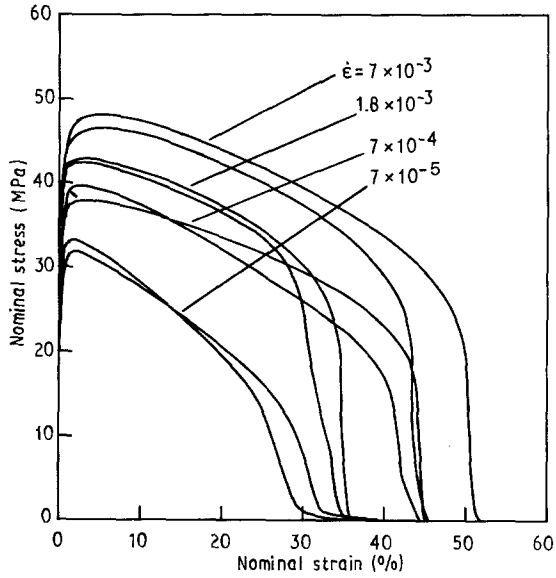

Figure 3 Nominal stress–strain curve (25 °C).

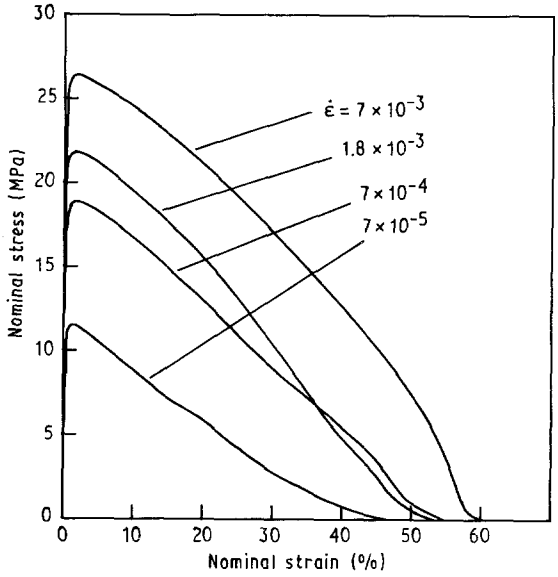

Figure 4 Nominal stress–strain curve (100 °C).

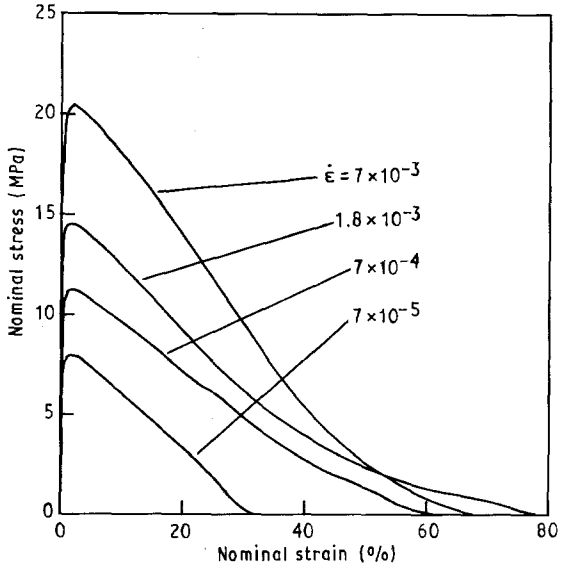

Figure 5 Nominal stress–strain curve (140 °C).

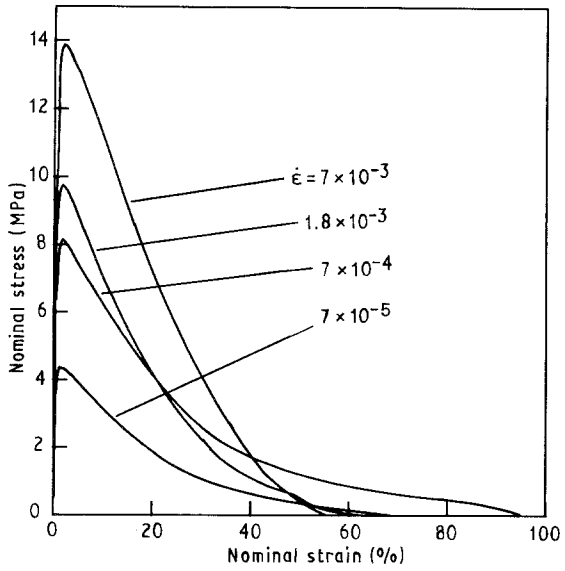

Figure 6 Nominal stress–strain curve (170 °C).

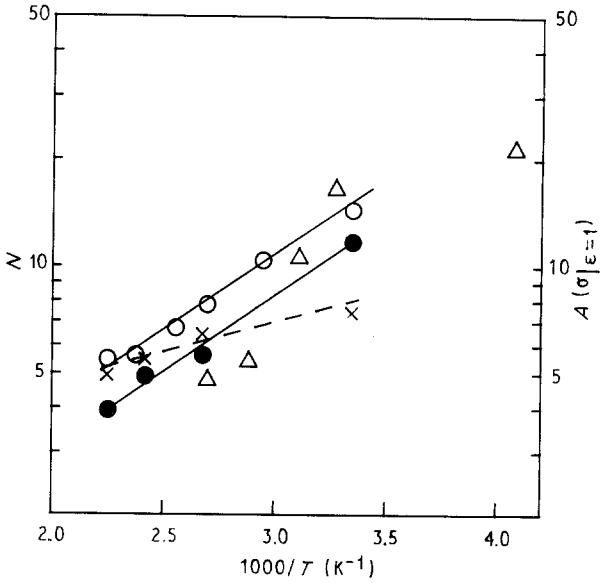

Figure 8 Temperature dependence of N and A. N: (●) Present results, (○) [11], (△) [4]. A: (×) Present results, at $\dot{\varepsilon} = 1\,s^{-1}$.

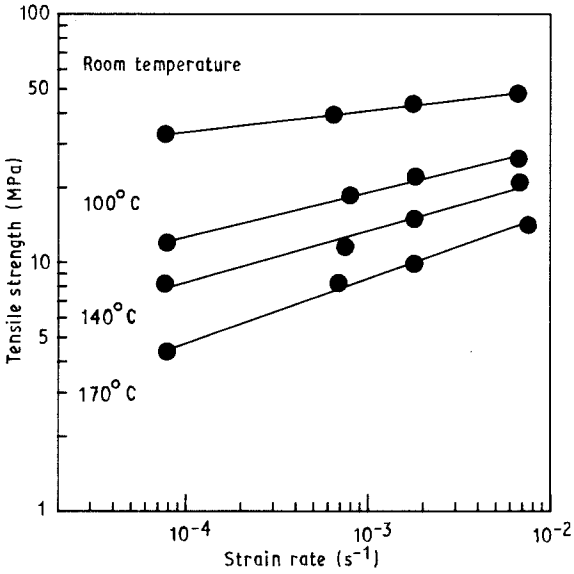

Figure 7 Effect of strain rate on tensile strength.

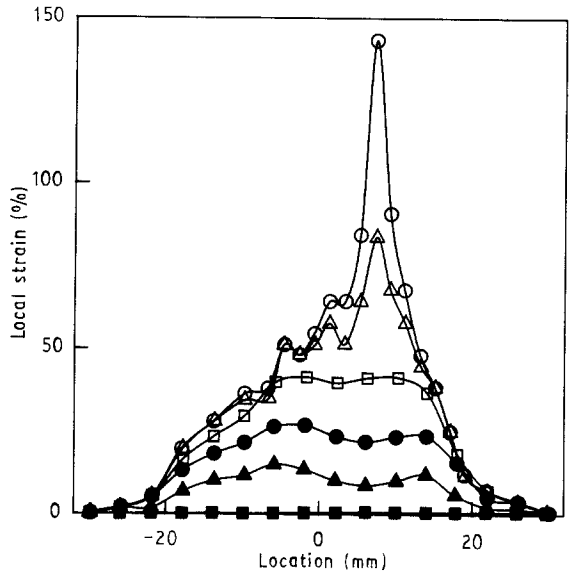

Figure 9 Local strain distribution. Nominal strain: (■) 2%, (▲) 10%, (●) 20%, (□) 30%, (△) 40%, (○) 45%.

steady creep that only the coefficient A depends on temperature but not on N, the slope of the lines in Fig. 7, the exponent, N, varies with temperature.

The change in the exponent N and coefficient A with temperature is shown in Fig. 8. In this figure, the experimental results are compared with those obtained from Kashyap and Murty ([11] Fig. 3) for the range $\dot{\varepsilon} > 0.001\,s^{-1}$, and the values given by Hall ([4] Table I). Those results were obtained for the eutectic Sn–Pb solder. From these results we can conclude that the exponents do depend on the temperature. If we admit some scattering of the data, N and A can be expressed by

$$N = 0.512 \exp(900/T) \quad (2)$$

$$A = 2.42 \exp(356/T) \quad (3)$$

The local strain distribution along the longitudinal axis of the specimen was obtained by measuring the change in the spacing of the grating drawn on its surface. Fig. 9 shows the result of the test at 25 °C and $\dot{\varepsilon} = 7 \times 10^{-4}\,s^{-1}$. The initial spacing of the grating was 1 mm, while the local strain was evaluated for every 4 and 2 mm after formation of necking. Up to a nominal strain of 20%, the distribution was fairly uniform within the parallel portion; however, a visible neck appeared over a nominal strain of 40%. The specimen fractured at 45% nominal strain, whereas the maximum local strain with 2 mm gauge length attained about 140%. This distribution is similar to that of highly pure eutectic solder [12] in Region III, whereas the magnitude of elongation in our test is about one-half that given by Ahmed and Langdon [12]. The difference may be attributed to grain-boundary embrittlement due to impurities. The macroscopic feature of the fractured specimen is shown in Fig. 10.

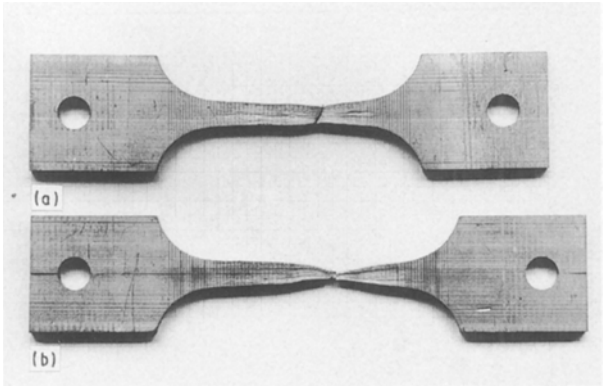

Figure 10 Fractured specimen: (a) 25 °C, (b) 170 °C.

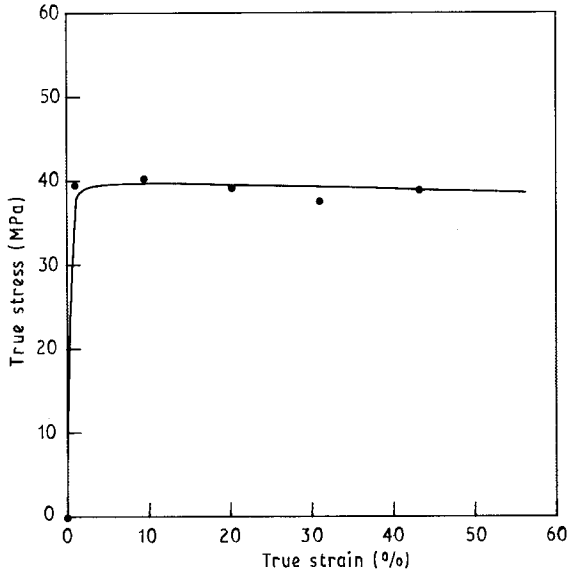

Figure 11 The true stress–strain curve (25 °C).

With the local strain shown in Fig. 9 and assuming material incompressibility, the true stress–strain curve was obtained for the test at 25 °C and $\dot{\varepsilon} = 7 \times 10^{-3}\,s^{-1}$, Fig. 11. This diagram shows slight work softening even on the true stress–strain plot. Similar results have been reported for a compression test by Kitamura *et al.* [10]. This softening is explained by recrystallization due to dynamic ageing [13].

For the magnitude of allowable strain for practical solder joints, however, the elastic perfectly plastic model can be applied for this solder.

4. Conclusions

1. Tensile tests of the cast Sn–Pb eutectic solder were performed at temperatures ranging from 25–170 °C and strain rates of 7×10^{-5}–$7 \times 10^{-3}\,s^{-1}$.

2. Nominal stress–strain curves attain a peak at a few per cent strain, and thereafter stress falls gradually due to diffusion of the neck.

3. The true stress–strain curve at room temperature shows slight strain softening, but it can be modelled by the elastic perfectly plastic body.

4. The tensile strength is expressed by a power function of strain rate whose exponent and coefficient are determined by a kind of Arrhenius' equation.

5. The empirical formula mentioned above gives a good estimation of the dependence of tensile strength on strain rate and temperature.

Acknowledgement

The authors thank Mr H. Kodama for technical assistance.

References

1. R. N. WILD, *Welding J.* **51** (1972) 521s.
2. H. D. SOLOMON, in "Low-cycle Fatigue ASTM STP942", edited by H. D. Solomon, G. R. Halford, L. R. Kaisand and B. N. Leis (ASTM, Philadelphia, PA, 1988) p. 342.
3. D. GRIVAS, K. L. MURTY and J. W. MORRIS Jr, *Acta Metall.* **27** (1979) 731.
4. P. M. HALL, *IEEE Trans. CHMT* **12** (1987) 556.
5. C. J. THWAITES and W. B. HAMPSHIRE, *Welding J.* **56** (1976) 323s.
6. N. F. ENKE, T. J. KILINSKI, S. A. SCHROEDER and J. R. LESNIAK, *IEEE Trans. CHMT* **12** (1989) 459.
7. E. R. BANGS and R. E. BEAL, *Welding J.* **55** (1975) 377s.
8. H. E. BOYER, "Atlas of stress-strain curves" (ASM International, Metals Park, OH, 1987).
9. R. SATOH, M. OHSHIMA, K. ARAKAWA and K. HIROTA, *J. Jpn Inst. Metals* **49** (1985) 26.
10. T. KITAMURA, S. KIKUCHI and M. KOIWA, *J. Soc. Mater. Sci. Jpn* **38** (1989) 989.
11. B. P. KASHYAP and G. S. MURTY, *Mater. Sci. Engng* **50** (1981) 205.
12. M. M. I. AHMED and T. G. LANGDON, *J. Mater. Sci.* **18** (1983) 2407.
13. K. LANGE, "Handbook of metal forming" (McGraw-Hill, New York, 1985) p. 3.21.

Received 16 July 1991
and accepted 17 February 1992